Ranging and Doppler Localization Using Golay Codes as the Phase Coding Signal

AAMIR HUSSAIN*, AND MUHAMMAD BILAL MALIK*

RECEIVED ON 19.05.2009 ACCEPTED ON 13.08.2009

ABSTRACT

In this paper we develop a signal processing algorithm for the detection, ranging and Doppler localization of moving target using Golay code as the phase coding signal. We exploit the side-lobes suppression property of Golay code, that occurs in complementary code pair, for side-lobe free target detection, range estimation and Doppler localization. Golay code based phase coding is achieved using QPSK (Quadrature Phase Shift Keying) scheme. When the transmitted signal is reflected from a moving target, its complex demodulation is carried out at the receiver. This is followed by correlation of each component of demodulated signal with one member of the complementary Golay code pair separately. The correlation results of the two channels are added together, leading to effective side-lobes suppression when phase and frequency of the demodulating carriers match with that of the received signal. The shift in the time index of the correlation peak gives the range to the target. Frequency of the demodulating carriers at which side-lobe free correlation peak occurs at the output indicates Doppler frequency corresponding to the target speed. The developed technique exhibits excellent Doppler localization, target detection and range estimation performance by overcoming the side-lobe limitations of the conventional phase coding signals in ranging applications.

Key Words: Correlation, Detection, Doppler Frequency, Golay Codes, Phase Coding, Range Estimation, Quadrature Phase Shift Keying, Side Lobe Suppression, Serial Search, Frequency Banks, Maximum Likelihood Estimation.

1. INTRODUCTION

Barker, PN, Kasami and Gold sequences are the conventional phase coding signals used in the ranging applications [1]. A continuous phase coded signal is transmitted in the direction where one or more targets are expected to be present. Target detection is carried out by correlating the received signal with the coding sequence at baseband [2-6]. The conventional coding signals have a problem that side-lobes appear in their correlation at the receiver [1]. These side-lobes may lead to false alarms and masking of weak targets [1].

Different approaches have been used for the side-lobe free detection and ranging. Ackroyd, et. al. [7] have presented an optimal inverse filtering technique for minimizing the ISL (Integrated Side-Lobe Level) in least square sense. Robert, et. al. [8] have proposed code inverse filtering for complete side-lobe removal. But the performance of matched filter as well as the inverse filter degrades in the presence of a Doppler shifted return of the signal [8]. Mudukutore, et. al. [9] use Pulse compression to improve range resolution while maintaining a high duty cycle. Bucci [10] has proposed a Doppler tolerant range side-lobe

*College of Electrical & Mechanical Engineering, National University of Science & Technology, Rawalpindi.

suppression scheme. Gurtz, et. al. [11] has Generated uniform amplitude complex code sets with low correlation side lobes. Suto, et. al. [12] have introduced a time side lobe reduction technique for binary phase code pulse compression. Xin, et. al. [13] have introduced a chaotic phase code for Radar Pulse compression. Kai, et. al. [14] discuss a new wave form with high range resolution. Chandrasekhar, et. al. [16] present waveform coding for dual polarization weather radars. Jorgan, et. al. [14] present azimuth phase coding for range ambiguity suppression. Shen, et.al.[16] propose window functions for reducing the side-lobe levels and obtaining high range resolution. James, et. al. [18] seek to minimize the estimation error of a range profile directly. Sune, et. al. [19-20] uses ultra wideband noise waveforms for side lobe suppression, and applies mismatched filtering to suppress the side-lobes of random noise radar.

Golay code is a pair of two complementary codes, code-c and code-k, each having length of 2^M, where M is a positive integer [22-24]. Golay codes have a remarkable property that addition of auto-correlation of the two complementary codes results in zero side-lobes [25-27]. This property of Golay codes is well-known in literature [23-25,27] and is useful in case of detection of multiple and weak targets [3,5]. Golay codes have traditionally been used for channel coding in digital communications [22-23]. In our previous work, we have applied Golay codes to base band ranging applications and some communications applications [28-29]. In this paper, we present side-lobe free ranging and Doppler localization of a moving target using Golay Code as the phase coding signal. In case of ranging applications, the index of the correlation peak gives the delay which corresponds to the range to the target [3-4].

Rest of the paper is organized as follows. In Section 2, we discuss detection of signals with unknown arrival time. The side-lobes suppression property of the Golay codes is discussed in Section 3. In Section 4, we discuss QPSK pass-band scheme to achieve Golay code based phase coded signal for transmission. In Section 5, we present the side-lobe free detection, ranging and Doppler localization algorithm for the Golay code based QPSK received signal. The received signal is the delayed and frequency shifted (due to target motion) version of the transmitted signal. We adopt a complex demodulation scheme for demodulating the received signal. A phase offset is introduced in the demodulating carriers at the receiver. In order to match phase and frequency of the demodulating carriers with that of the received signal, serial search strategy is adopted. The in-phase component of the demodulated signal is correlated with code-c and the quadrature component with code-k. The auto-correlation results of the two channels are added together, leading to effective side-lobes suppression when phase and frequency of the demodulating carriers match with that of the received signal. Frequency of the demodulating carriers then equals the Doppler frequency that corresponds to the speed of the target. The side-lobe free correlation peak occurs at a delay corresponding to the range of the target. Computer simulations demonstrate usefulness of the ideas presented. In Section 6, two other efficient approaches to frequency and phase matching are discussed very briefly i.e. parallel frequency banks and the MLE (Maximum Likelihood Estimation) technique. In Section 7, the detection performance of the detector for the detection of Golay code based QPSK transmitted signal is discussed. Concluding remarks are given in Section 8.

2. DETECTION OF SIGNALS WITH UNKNOWN ARRIVAL TIME

Golay code based phase coded signal is transmitted continuously in a specific direction. Echo with a delay is received from the target by the receiver placed besides the transmitter. This is the problem of detecting a signal with unknown arrival time [2-4]. This delay is detected by correlating the received signal with the code sequence at baseband [3-4]. Hence, a GLRT (Generalized Likelihood Ratio Test) can be employed as a detector/estimator [2,4]. We consider following two hypotheses:

H_0: x[n] = w[n]   n = 0,1.....N-1 (1)

H_1: x[n] = s[n-n_0] + w[n]   n=0,1.....N-1

where s[n] is a known deterministic signal that is non-zero over the interval [0,m-1], n_0 is the unknown delay, and w[n] is WGN (White Gaussian Noise) with zero mean and variance σ^2. H_0 is the noise-only hypothesis, whereas H_1 is the noise-plus-signal hypothesis. Clearly the observation interval [0,N-1] should include the signal for all possible delays. A GLRT would decide H_1 [3] if following inequality holds:

$$\frac{p\left(x;\hat{n}_O,H_1\right)}{p\left(x;H_0\right)} > \gamma$$

where $\hat{n}_O$ is the MLE of n_0 [2-4]. $p(x;\hat{n}_O,H_1)$ is the PDF of x under H_1 and p(x;H_0) is the PDF of x under H_0. $\hat{n}_O$ is found by maximizing Expression (Equation (2)) over all possible n_0 [2-4].

$$\sum_{n=n_0}^{n_0+M-1} x\left[n\right]s\left[n-n_0\right] \tag{2}$$

The received signal, after complex demodulation, is correlated with all possible delayed signals and $\hat{n}_O$ is chosen to be the value that maximizes Expression (Equation (2)). In case of H_1, Expression (2) becomes [3]:

$$\sum_{n=\hat{n}_0}^{\hat{n}_0+M-1} x\left[n\right]s\left[n-\hat{n}_0\right] \geq \gamma' \tag{3}$$

Expression (Equation (3)) shows the correlation of x[n] with $[n-\hat{n}_0]$. The maximum value of correlation is obtained at $n-\hat{n}_0$, which is compared with a threshold γ'. If the threshold is exceeded, a signal (target) is declared to be present and its delay (range) is estimated as $\hat{n}_O$; otherwise noise only is declared [2,4].

3. SIDE-LOBE SUPPRESSION PROPERTY OF GOLAY CODE

Golay code is a pair of complementary codes (say code-c and code-k) [21-26]. When the autocorrelation results of the codes of a complementary Golay code pair are added, the side-lobes in the two correlation results being complementary to each others are canceled and hence completely suppressed [21-27]. We demonstrate this side-lobe suppression by using a complementary Golay code pair of length 64. Auto correlation of the two members of the complementary Golay code pair of length 64 are given in Figs. 1-2. When the correlation results of Figs. 1-2 are added, the side-lobes are completely suppressed as shown in Fig. 3. In the ranging applications, the final display of the target range is on a 1-to-M samples map as shown in Fig. 4. M is the length of individual code.

4. GOLAY CODE BASED QPSK TRANSMISSION

A pass-band communication scheme is adopted for Doppler localization application. We use the QPSK scheme for transmitting both the codes of the complementary Golay code pair in the pass band; and to achieve the Golay code based phase coded signal. Code-c is used to modulate the in-phase carrier cos(ω_cn), whereas

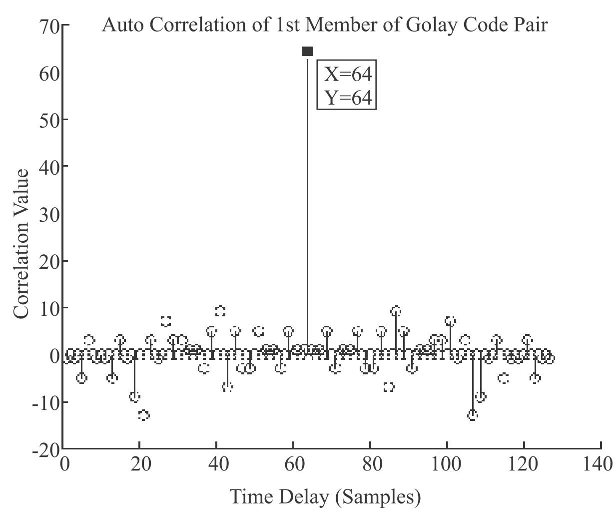

FIG. 1. AUTO-CORRELATION OF CODE-C OF GOLAY CODE PAIR

code-k is used to modulate the quadrature carrier $\sin(\omega_c n)$. These two BPSK modulated signals are added which gives the Golay code based phase coded QPSK signal for transmission as depicted in Fig. 5. The transmitted QPSK signal is [6,30].

$$s[n] = c[n]\cos(\omega_c n) + k[n]\sin(\omega_c n) \tag{4}$$

5. TARGET DETECTION AND RANGING

5.1 Framework

Echo is received by the receiver with delay n_0 from an approaching target with velocity corresponding to Doppler frequency ω_D. The carrier frequency is shifted from ω_c to $\omega_c+\omega_D$ and some phase distortion ϕ is introduced in the received signal due to the channel effect and delay n_0. The signal received at the receiver is given by [6]:

$$r[n]=c[n-n_0]\cos((\omega_c+\omega_D)n+\phi)+k[n-n_0]\sin((\omega_c+\omega_D)n+\phi) \tag{5}$$

Where ϕ is a function of the target delay n_0. The receiver for the Golay code based QPSK transmitted signal is given in Fig. 6. We have adopted complex demodulation scheme for processing the received signal. The received signal r[n] is demodulated by the in-phase carrier $\cos(\omega_n)$, and the quadrature-phase carrier $\sin(\omega_n)$ [6]. For Doppler localization of the moving target we vary the frequency of both the demodulating carriers simultaneously from

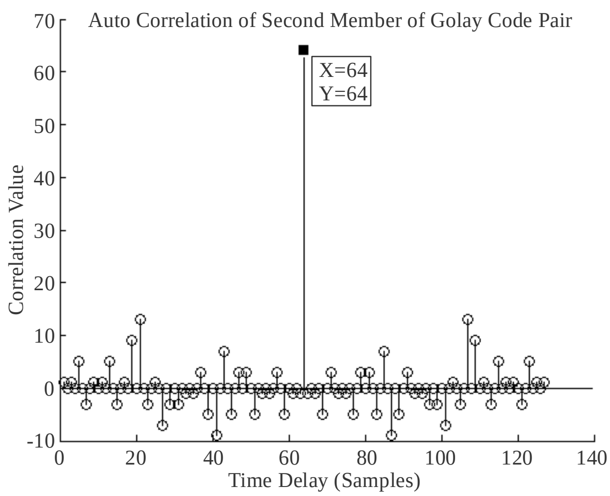

FIG. 2. AUTO-CORRELATION OF CODE-K OF GOLAY CODE PAIR

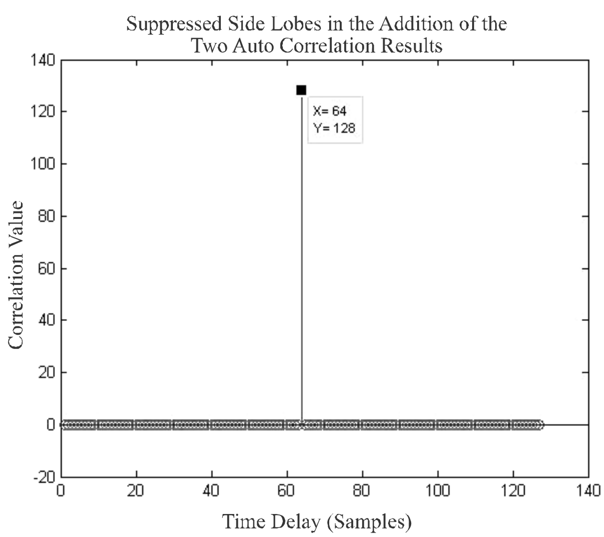

FIG. 3. SUPPRESSED SIDE LOBES IN THE ADDITION OF CORRELATION RESULTS OF COMPLEMENTARY PAIR

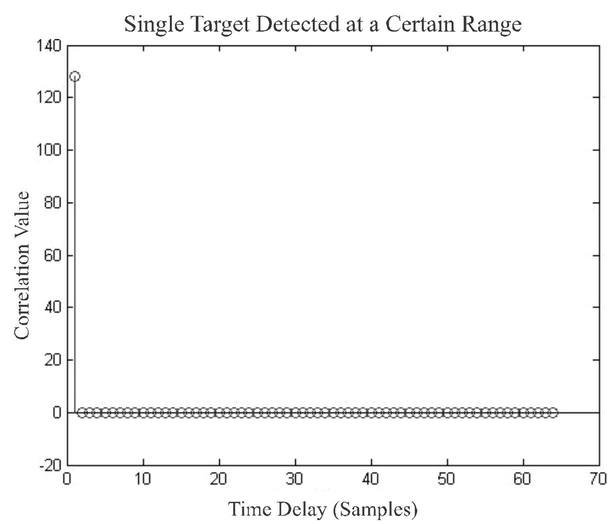

FIG. 4. FINAL DISPLAY OF THE TARGET RANGE ON A 1-M SAMPLES MAP

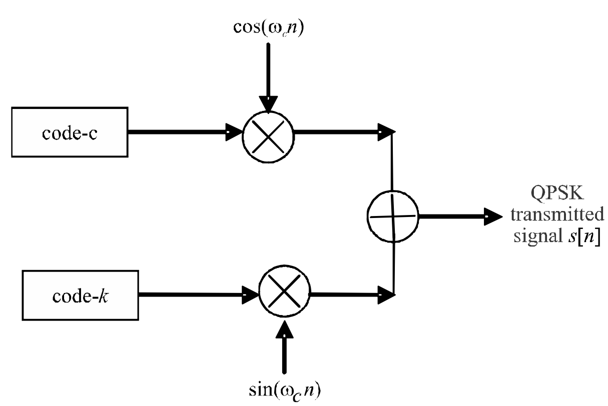

FIG. 5. GOLAY CODES BASED QPSK TRANSMISSION

ω_c-ω_{Dmax} to ω_c+ω_{Dmax} in increments of frequency $\Delta\omega$ until we reach the frequency ω_c+ω_D. ω_{Dmax} is the pre-defined maximum Doppler frequency which can be handled. In case of a receding (opening) target, the corresponding frequency of the received signal is ω_c-ω_D.

In Fig. 6, LPF stands for low pass filtering. To cater for the phase ϕ introduced by the channel into the received signal, a phase offset $\hat{\phi}$ is introduced in the demodulating carriers. For each frequency of both the demodulating carriers, the phase offset $\hat{\phi}$ is varied sequentially from 0-2π. The reason for introducing this phase offset into the demodulating carriers will be explained later. After low pass filtering, we correlate (at base band) the in-phase component of demodulated signal with code-c, and the quadrature-component of demodulated signal with code-k. The two correlation results are added. When the frequency and phase of both the demodulating carriers matches to the frequency and phase of the received signal r[n], we get a side-lobe free delta function at a delay $\hat{n}_0$ [2,5]. $\hat{n}_0$ is the MLE of the delay n_o corresponding to the range of the target [2].

When the frequencies of both the demodulating carriers match the frequency of the Doppler shifted received signal i.e. ω_c+ω_D, the in-phase component of the complex demodulation is [6] given by:

$$r_1\left[\hat{n}_0\right] = c\left[n-n_0\right]\left[\cos\left(\left(\omega_c+\omega_D\right)n+\phi\right)\right] + k\left[n-n_0\right]\left[\left(\sin\left(\omega_c+\omega_D\right)n+\phi\right)\right]$$
$$\left[\cos\left(\left(\omega_c+\omega_D\right)n+\hat{\phi}\right)\right] r_1\left[\hat{n}_0\right] = c\left[n-n_0\right]\left[\cos\left(\phi+\hat{\phi}\right)+\cos\left(2\left(\omega_c+\omega_D\right)n+\phi+\hat{\phi}\right)\right]$$
$$+k\left[n-n_0\right]\left[\left[\sin\left(\phi-\hat{\phi}\right)\right]+\sin\left(2\left(\omega_c+\omega_D\right)n+\phi+\hat{\phi}\right)\right] \quad (6)$$

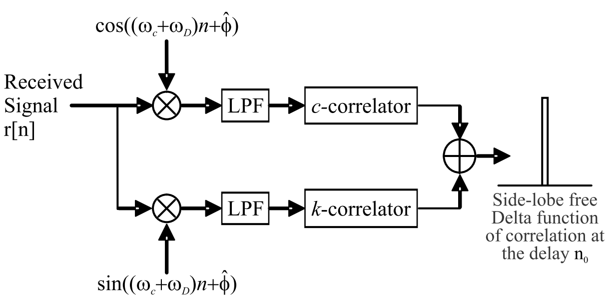

FIG. 6. DEMODULATION SCHEME AND THE CORRELATION AND ADDITION ALGORITHM

And the quadrature-component of the complex demodulation is [6] given by:

$$r_0\left[\hat{n}_0\right] = c\left[n-n_0\right]\left[\cos\left(\omega_c+\omega_D\right)n+\phi\right] + k\left[\left[n-n_0\right]\left(\sin\left(\omega_c+\omega_D\right)n+\phi\right)\right]$$
$$\left[\sin\left(\left(\omega_c+\omega_D\right)n+\hat{\phi}\right)\right] \hat{r}_0\left[\hat{n}_0\right] = c\left[n-n_0\right]\left[\sin\left(\phi+\hat{\phi}\right)+\sin\left(2\left(\omega_c+\omega_D\right)n+\phi+\hat{\phi}\right)\right]$$
$$+k\left[n-n_0\right]\left[\left[\cos\left(\phi-\hat{\phi}\right)\right]+\cos\left(2\left(\omega_c+\omega_D\right)n+\phi+\hat{\phi}\right)\right] \quad (7)$$

The high frequency terms in Equations (6) and (7) are filtered out by the low pass filters:

$$r_1\left[\hat{n}_0\right] = c\left[n-n_0\right]\cos\left(\phi-\phi\right) + k\left[n-n_0\right]\sin\left(\phi-\hat{\phi}\right) \quad (8)$$

$$r_Q\left[\hat{n}_0\right] = c\left[n-n_0\right]\sin\left(\phi-\phi\right) + k\left[n-n_0\right]\cos\left(\phi-\hat{\phi}\right) \quad (9)$$

Correlation of the in-phase component is carried out with code-c at baseband which gives following result [30]:

$$y_Q\left[\hat{n}_0\right] = \sum_{n=\hat{n}_0}^{\hat{n}_0+M-1} c\left[n-n_0\right]k\left[n-\hat{n}_0\right]\sin\left(\phi-\phi\right)$$
$$+\sum_{n=\hat{n}_0}^{\hat{n}_0+M-1} k\left[n-n_0\right]c\left[n-\hat{n}_0\right]\sin\left(\phi-\hat{\phi}\right) \quad (10)$$

Here y_1 is the correlation value. The first term on the right side of Equation (10) is the correlation of code-c with itself. The second term is the cross-correlation of code-c with code-k [30]. We denote it by $y(c_n, k_{n-n0})$.

Correlation of the quadrature-component is carried out with code-k which results in [30]:

$$y_Q\left[\hat{n}_0\right] = \sum_{n=\hat{n}_0}^{\hat{n}_0+M-1} c\left[n-n_0\right]k\left[n-\hat{n}_0\right]\sin\left(\phi-\hat{\phi}\right)$$
$$+\sum_{n=\hat{n}_0}^{\hat{n}_0+M-1} k\left[n-n_0\right]k\left[n-\hat{n}_0\right]\cos\left(\phi-\hat{\phi}\right) \quad (11)$$

Here y_Q is the correlation value. The first term on the right side of Equation (11) is the cross-correlation of code-k with code-c. We denote it by $y(k_n,c_{n-n0})$. The second term is the auto-correlation of code-k with itself.

To get rid of the cross correlation terms in the correlation results of in-phase signal (Equation 10) and the quadrature-phase signal (Equation 11) is a challenging task. We proceed as follows. We add the two correlation results (Equation 10 and 11) and get Equation (12).

$$y\left[\hat{n}_0\right] 2M\delta\left[n-\hat{n}_0\right]\cos\left(\phi-\hat{\phi}\right)+\left[y\left(c_n, k_{n-n_0}\right)+y\left(k_n, c_{n-n_0}\right)\right]\sin\left(\phi-\hat{\phi}\right) \quad (12)$$

Here M is the code length of each Golay code member in the complementary pair.

In Equation (12), $y(c_n,k_{n-n0})$, $y(k_n,c_{n-n0})$ are the two cross correlation terms of Equation (10) and (11) respectively. In Equation (12), we get a delta function $\delta[n-\hat{n}_0]$ having amplitude $2M\cos(\phi-\hat{\phi})$ and the addition of the cross-correlation terms scaled with . When frequency and phase of the demodulating carriers matches with that of the received signal, the cross correlation terms in the correlation (Equation 12) become zero and we get a perfect delta function at a delay n_0 given by:

$$y\left[\hat{n}_0\right] 2M\delta\left[n-\hat{n}_0\right] \quad (13)$$

Equation (13) states that the correlation undertaken by GLRT has maximum value (correlation peak) at $n-\hat{n}_0$ [2]. This maximum value of correlation is compared to a threshold. In case of the presence of a target, the threshold is exceeded. A signal (target) is declared to be present and its delay (range) is estimated as $\hat{n}_0$ [2]. Otherwise noise only is declared. Thus the delay $(n-\hat{n}_0)$ corresponding to the range to the target and the Doppler frequency corresponding to its speed are determined using the side-lobe suppression property of the Golay code by following the demodulation, correlation and addition algorithm.

5.2 Simulation Results

We demonstrate the performance of proposed algorithm for side-lobe free detection, ranging and Doppler localization of a moving target using Golay code as the phase coding signal by using computer simulations. Here simulations are presented for a maximum range of 5m (ultrasonic environment). Length (M) of each code of the complementary Golay Code pair used for phase coding the carrier signal is 256.

Chip Time $T_c = 0.13\text{x}10^{-9}$ sec.

Repetition Period is $T = MT_c = 256\text{x}0.1310^{-9} = 3.58\text{x}10^{-8}$ sec.

Maximum Range R = CT/2= 5m (Here C is the speed of light).

Range Resolution = Maximum Range/Length of the coding sequence = 5/256 = 1.9cm.

Hence 1 sample delay = 1.9cm range.

An approaching target with velocity corresponding to a Doppler frequency ω_D is assumed to be present at a range of 0.9765 m from the receiver. It is also assumed that a phase offset $\omega=\pi/4$ has been introduced in the Golay code based QPSK received signal.

Time delay corresponding to 0.9765 m range is $\Delta=6.5\text{x}10^{-9}$ seconds = 50 samples delay.

Hence delay introduced in the received signal is $n_0=50$ samples which is to be found. We vary the frequency of the demodulating carriers serially from ω_c to $\omega_c+\omega_D$ in increments of equal frequency length. For each selected frequency of both the demodulating carriers, the self introduced phase at the demodulating carriers is varied from 0-2π in equal increments of $\pi/16$ each. When frequency of both the demodulating carriers matches the frequency of the Doppler introduced received signal i.e. $\omega_c+\omega_D$, after following the demodulation, correlation and addition algorithm at the receiver the resultant signal corresponds to Equation (12). In Equation (12)

ϕ=Phase distortion in the signal due to the channel effect and target delay.

$\widehat{\phi}$=Self introduced Phase into the demodulating carriers.

The simulation results are as under.

5.2.1 Case-1 $\phi = \pi/4, \widehat{\phi} = \pi/16$

Correlation of the in-phase component of demodulated signal (Equation 10) with code-c is given in Fig. 7. Correlation of quadrature-component of the demodulated signal with code-k (Equation 11) is given in Fig. 8. And the addition of the two correlation results (Equation 12) is shown in Fig. 9.

It can be observed that as the difference between ϕ and $\widehat{\phi}$ decreases the level of side -lobes reduces in the final correlation result.

5.2.2 Case-2 $\phi = \pi/4, \widehat{\phi} = 4\pi/16$

The addition of the two correlation results (Equation 12) for this case is given in Fig. 10.

5.2.3 Case-3 $\phi = \pi/4, \widehat{\phi} = 3\pi/16$

The addition of the two correlation results for this case is given in Fig. 11.

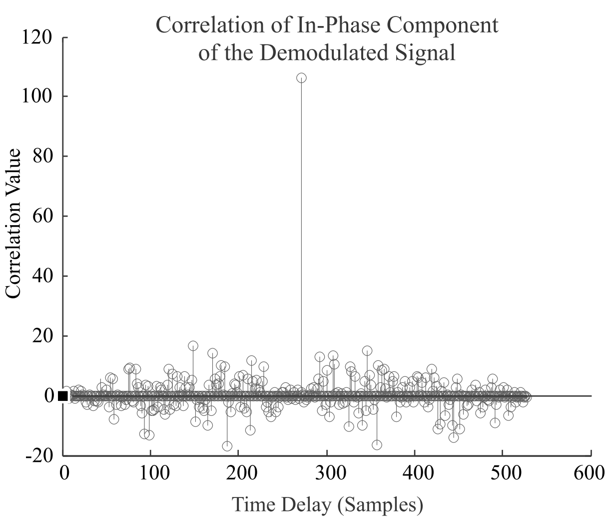

FIG. 7. CORRELATION OF IN-PHASE COMPONENT OF DEMODULATION WITH CODE-C

It can be observed that as the difference between ϕ and $\widehat{\phi}$ decreases the level of side -lobes reduces in the final correlation result.

5.2.4 Case-4 $\phi = \pi/4, \widehat{\phi} = 4\pi/16$

The addition of the two correlation results is given in Fig. 12. Here it is clearly seen that as $\widehat{\phi} = \phi$, the side-lobes are completely suppressed. So the main lobe of correlation is left whose time index gives the round trip delay $\widehat{n}_0$ corresponding to the range to the to the target range. When the difference between ϕ and $\widehat{\phi}$ increases,

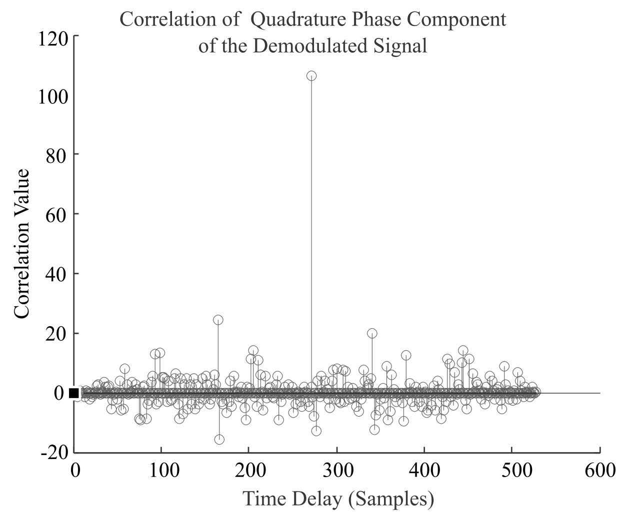

FIG. 8. CORRELATION OF QUADRATURE-COMPONENT OF DEMODULATION WITH CODE-K

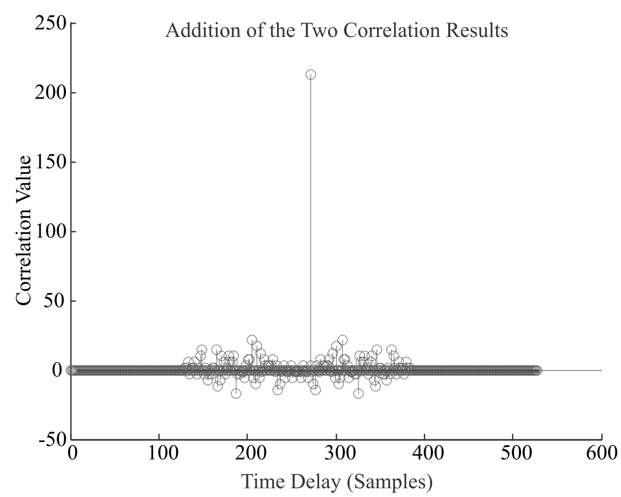

FIG. 9. ADDITION OF THE TWO CORRELATION RESULTS (CORRELATIONS OF FIG.7 AND FIG.8)

the level of side-lobes in the final result increase. It is to be noted that after following the demodulation, correlation and addition algorithm, a side lobe free delta function of correlation occurs at a delay $(\hat{n}_0)$ if and only if the frequency and phase of the demodulating carriers matches with that of the Doppler introduced received signal. The final display of the target range will be on a 1-256 samples map as shown in Fig. 13. The signal strength reduces proportionally after reflecting from a weak target (a distant or small irregular target). Detection and ranging of a 75% weak target is shown in Fig. 14.

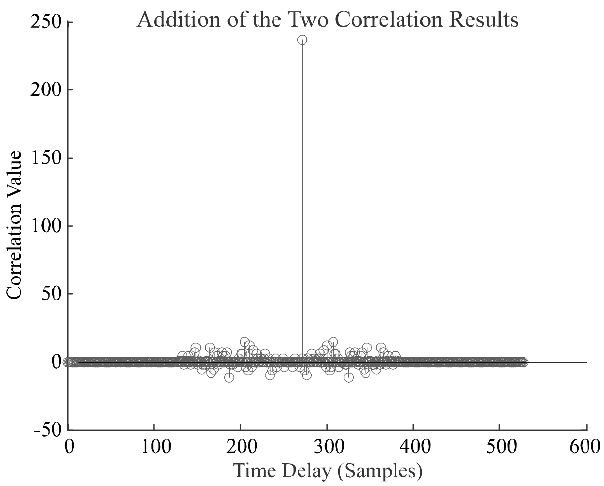

FIG. 10. ADDITION OF THE TWO CORRELATION RESULTS

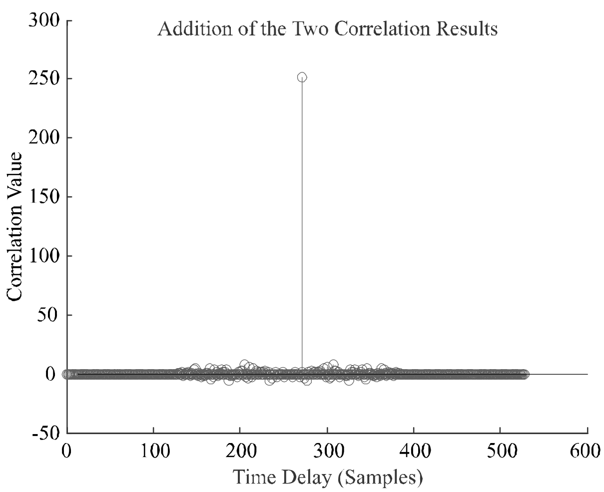

FIG. 11 . ADDITION OF THE TWO CORRELATION RESULTS

6. ALTERNATE APPROACH TO FREQUENCY AND PHASE ESTIMATION

Serial search strategy, discussed in preceding Section, for the frequency and phase is a time consuming technique since we have to try many combinations of frequency and phase. Efficient techniques for frequency and phase estimation exist in literature. We can use parallel frequency banks technique and the MLE of the phase as the fast variants of the serial search technique. We discuss them here briefly.

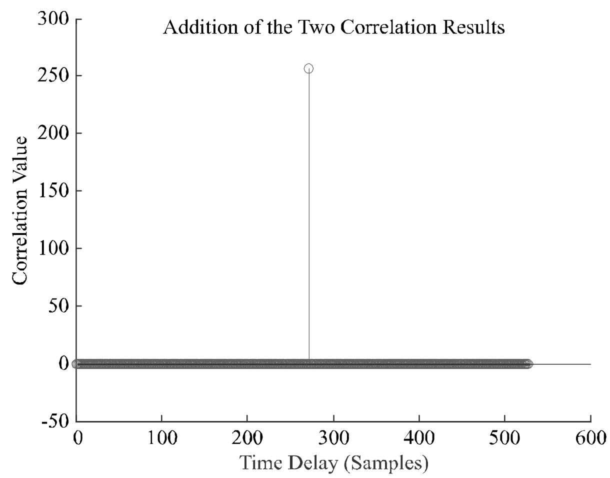

FIG. 12. ADDITION OF THE TWO CORRELATION RESULTS

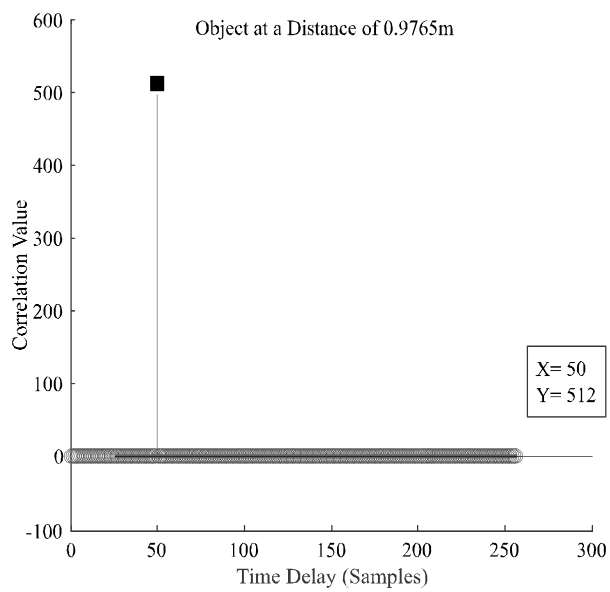

FIG. 13. DELAY OF THE OBJECT PRESENT AT 0.9765 M

6.1 The Parallel Frequency Banks Technique

In this technique we place the demodulation, correlation and addition block (DCA-Block of Fig. 6) in a number of times in parallel. Each DCA block has a unique frequency of the two demodulating carriers. The difference in frequency of the demodulating carriers of two consecutive DCA blocks is $\Delta\omega$. Phase of the demodulating carriers is varied from 0-2π at each DCA block. The incoming signal is introduced to all of the DCA blocks simultaneously, as shown in Fig. 15. The DCA block whose frequency matches the frequency of the Doppler introduced received signal gives delta function of correlation with suppressed side lobes at its output when $\hat{\phi} = \phi$. This technique is efficient as compared to the serial search strategy. However, more hardware resources are required for this technique.

6.2 MLE of the Phase of the Received Signal

In this approach, we find the MLE of the phase of the received signal. Then we introduce a phase offset equal to the MLE of the phase of the received signal simultaneously at the both the demodulating carriers of the DCA Block (Fig. 6) to get the side-lobe free delta function of correlation.

6.2.1 Finding MLE of Phase of the Received Signal

After demodulating the received signal r[n] with the in-phase and quadrature-phase carriers (without introducing the phase) followed by correlation with code-c and code-k respectively (Fig. 16), the maximum value of each correlation and its index is picked. The MLE of the carrier phase is found by the following relation [6].

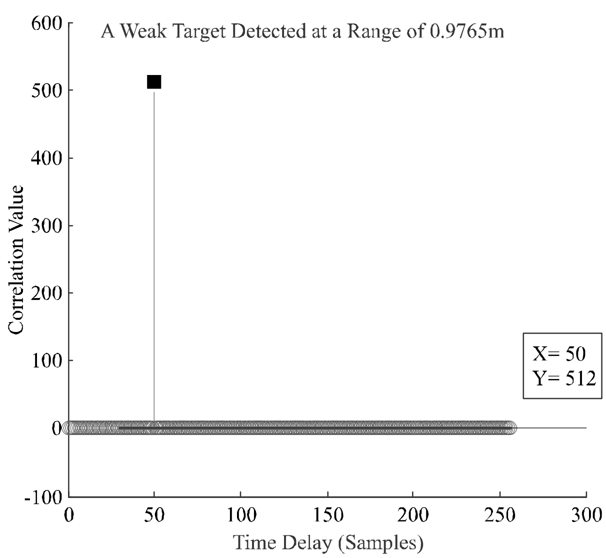

FIG. 14. DETECTION AND RANGING OF A WEAK TARGET

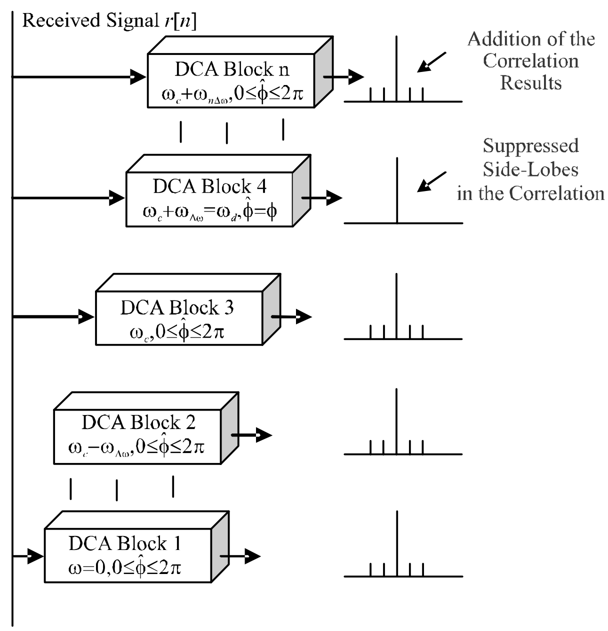

FIG. 15. PARALLEL FREQUENCY BANKS TECHNIQUE FOR FINDING THE FREQUENCY OF THE DOPPLER INTRODUCED RECEIVED SIGNAL

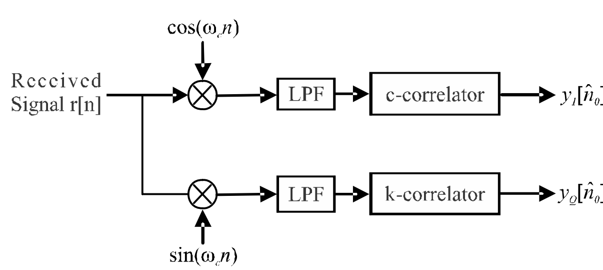

FIG. 16. FINDING MLE OF PHASE OF THE RECEIVED SIGNAL
FIG. 17. INTRODUCING MLE OF THE PHASE INTO THE

$$\text{MLE of Phase} = \hat{\phi} = -\tan^{-1}\left(\frac{\max y_Q[\hat{n}_0]}{\max y_1[\hat{n}_0]}\right) \tag{14}$$

where $y_1[\hat{n}_0]$ and $y_Q[\hat{n}_0]$ are the correlation values given by:

$$y_1[\hat{n}_0] = \sum_{n=\hat{n}_0}^{\hat{n}_0+M-1} c[n-n_0]c[n-\hat{n}_0][\cos(\omega_D n+\phi)] + \sum_{n=\hat{n}_0}^{\hat{n}_0+M-1} k[n-n_0]c[n-\hat{n}_0][\sin(\omega_D n+\phi)] \tag{15}$$

$$y_Q[\hat{n}_0] = \sum_{n=\hat{n}_0}^{\hat{n}_0+M-1} c[n-n_0]k[n-\hat{n}_0][\sin(\omega_D n+\phi)] + \sum_{n=\hat{n}_0}^{\hat{n}_0+M-1} c[n-n_0]k[n-\hat{n}_0][\cos(\omega_D n+\phi)] \tag{16}$$

6.2.1 Using MLE of the Phase of the Received Signal

After finding the MLE of the phase of the received signal, the demodulating carriers at the receiver are given phase offset by an amount $\hat{\phi}$ as found using Equation (14). Fig. 17 shows how $\hat{\phi}$ is used by the receiver. MLE of phase of the received signal can be introduced simultaneously to the demodulating carriers of all the DCA blocks of Fig. 15.

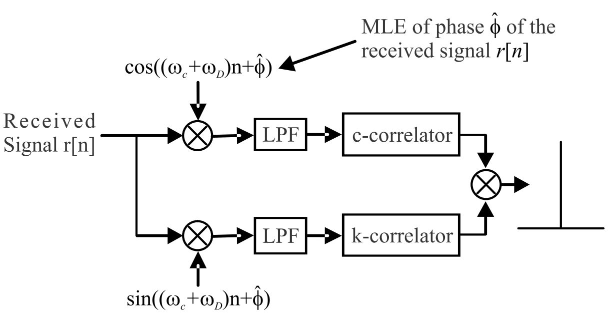

DEMODULATING CARRIERS OF A DCA BLOCK AT THE RECEIVER

FIG. 18. ROC OF THE RECEIVER FOR THE DETECTION OF

7. Receiver Operating Characteristics of the Receiver

The detection performance of a detector is the plot of detection probability versus probability of false alarm [3]. Performance of detector for the detection of phase coded signal with Golay code is evaluated for three different ENR (Energy to Noise Ratio), and the results are presented in Fig. 18.

The ROC (Receiver Operating Characteristics) shows that P_D increases with decrease in noise variance. This shows a very good detection performance of the detector for the Golay code based received signal [3].

7.1 Results and Discussion

The unconventional use of Golay codes in ranging applications by exploiting their side-lobe suppression property, the effective use of the QPSK scheme to achieve phase coding and pass-band transmission of both the complementary codes on the same signal are innovative research ideas. Furthermore, the development of the demodulation, correlation and addition algorithm for pass-band Doppler localization, detection and side -lobe free

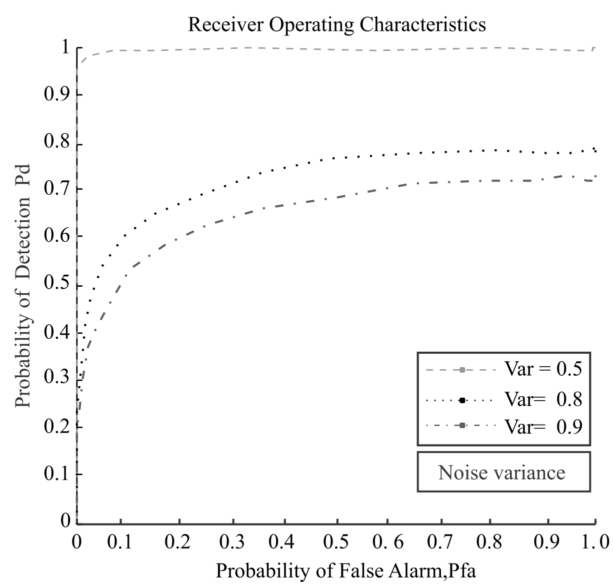

GOLAY CODE BASED PHASE CODED SIGNAL WHEN NOISE IS WHITE ranging (Equation 12) are very useful research contributions made in this paper. The demodulation scheme is intelligently used for Doppler localization by following the correlation and addition algorithm. Use of phase offset $\hat{\phi}$ at the demodulating carriers is yet another effective use of the parameters of the demodulating signal to cancel the cross-correlation side-lobes in the final correlation result (Equation 12). For efficient execution of the algorithm, the parallel frequency banks and the MLE of the phase of the received signal are discussed very briefly as the possible variants of the basic serial search strategy. Even much efficient and accurate estimation techniques for the frequency and phase of the received signal can be adopted. In our algorithm, estimation of Doppler frequency and phase of the received signal are achieved as the necessary conditions in the complete execution of the algorithm. This signal processing algorithm is a new addition in the Doppler localization, side-lobe free detection and ranging applications for example civil defense radar. Furthermore, its application may be found in some of the important mobile communications problems such as carrier phase recovery when the receiver (mobile phone set) is in motion. With its sound mathematical basis, Golay code based QPSK scheme and the signal processing algorithm are expected to become an important tool in Doppler localization, detection and ranging applications.

8. CONCLUSION

We have seen that the development of Golay code based QPSK Scheme and the detection and ranging algorithm (Equation 12) has overcome the side-lobe limitations of the conventional coding signals in ranging applications i.e. of Barker, Kasami, PN and Gold Sequences etc. Doppler localization is achieved as a necessary condition in the complete execution of the ranging algorithm. Side-lobe free delta function of correlation is achieved at the output of the receiver at a delay $(\hat{n}_0)$ when the frequency and phase of the demodulating carriers match with frequency and phase of the Golay code based received signal. Parallel frequency banks and the MLE of the phase of the received signal can accelerate the execution of the algorithm. This new scheme and signal processing algorithm exhibits good Doppler localization and ranging capability, and the detector for Golay code based QPSK signal exhibits excellent detection performance. Our work furnishes sufficient details so as to make the basic theory of Doppler localization and side-lobe free detection and ranging using Golay Codes clear and ready to be used by a designer. The theory is expected to attract a much wider area of research in the future. It will give rise to new algorithms and solutions for a diverse range of estimation/ detection, ranging and Doppler localization problems especially in case of detection and ranging of weak targets.

ACKNOWLEDGMENTS

The authors are thankful to their colleague Dr. Muhammad Salman, for valuable comments for its improvement. The Reviewer's efforts are also acknowledged as it helped in improving the paper. The authors also acknowledge Higher Education Commission, Pakistan, for the support received from them under Ph.D. scholarship grant.

REFERENCES

[1] Barton, D.K., “Modern Radar System Analysis”, Artech House Inc., 1988.

[2] Kay, S.M., “Fundamentals of Statistical Signal Processing: Estimation Theory”, Volume I, Chapter-7, pp. 157 Prentice-Hall, Upper Saddle River NJ, USA, 1993.

[3] Kay, S.M., “Fundamentals of Statistical Signal Processing: Detection Theory”, Volume II, Chapter-7, pp. 260 Prentice-Hall, Upper Saddle River, NJ, USA, 1998.

[4] Barkat, M., “Signal Detection and Estimation”, 2nd Edition, Chapter-10, pp. 533, Artech House Inc., 2005.

[5] Hayes, M.H., “Statistical Digital Signal Processing and Modeling”, John Wiley & Sons (Asia) Pte. Ltd., Singapore, 2003.

[6] Haykin, S., “Communication Systems”, 4th Edition, Chapter-6, pp. 354-364, John Wiley and Sons, 2001.

[7] Ackroyd, M.H., and Ghani, F., "Optimum Mismatched Filters for Side Lobe Suppression", IEEE Transactions Aerospace & Electronic Systems, Volume 36, pp. 214-218, March, 1993.

[8] Daniels, R.C., and Gregers-Hansen, V., "Code Inverse Filtering for Complete Side-Lobe Removal in Binary Pulse Compression Systems", IEEE International Radar Conference, pp. 256-261, 9-12 May, 2005.

[9] Mudukutore, A.S., Chandrasekhar, V., and Keller, R., "Pulse Compression for Weather Radars", IEEE Transactions on Geoscience and Remote Sensing, Volume 36, No.1, pp. 125-142, January, 1998.

[10] Bucci, N.J., "Doppler Tolerant Range Side-Lobe Suppression for Pulse Compression Radars", Technical Reference MTMR-TR-001, GE Aerospace, Moorestown NJ, IEEE 1992 (Paper Downloaded from IEEE Explore).

[11] Gurtz, K.J., "Generation of Uniform Amplitude Complex Code Sets with Low Correlation Side Lobes", IEEE Transactions on Signal Processing, Volume 40, No. 2, pp. 343-353, February, 1992.

[12] Suto, R., and Shinriki, M., "Time Side Lobe Reduction Technique for Binary Phase Coded Pulse Compression", IEEE International Radar Conference, pp. 809-814, Alexendaria,VA, USA, 7-12 May, 2000.

[13] Wu, X., Liu, W., Zhao, L., and Fu, J.S., "Chaotic Phase Code for Radar Pulse Compression", Proceedings of the IEEE Radar Conference, pp. 279-283, 1-3 May, 2001.

[14] Kai, J., Wei-Dong, W., and Jin, W.D., "The Study of New Radar Wave form with High Range Resolution", IEEE International Conference on Signal Processing, pp. 1957-1960, 2004.

[15] Dall, J., and Kusk, A., "Azimuth Phase Coding for Range Ambiguity Suppression in SAR", IEEE International Geoscience and Remote Sensing Symposium, pp. 1734-1737, 20-24 September, 2004.

[16] Chandrasekhar, V., Bharadivy, N., and George, J., "Waveform Coding for Dual Polarization Weather Radars", IEEE International Geoscience and Remote Sensing Symposium, pp. 3571-3574, 23-28 July, 2007.

[17] Shen, H., Zhang, W., Kwak, K.S., "The Modified Chirp UWB Ranging System for Vehicular Applications", IEEE International Symposium on Communications and Information Technologies, pp.1038-1042, 17-19 October, 2007.

[18] Jenshak, J.D., and Stils, J.M., "A Fast Method for Designing Optimal Transmit Codes for Radar", IEEE Radar Conference, pp.1038-1042, 26-30 May, 2008.

[19] Anelson, S.R.J., "Random Noise Radar/Sonar with Ultra Wideband Waveforms", IEEE Transactions on Geo Science and Remote Sensing, Volume 45, No. 5, pp. 1099-1114, May, 2007.

[20] Anelson, S.R.J., "Suppression of Noise Floor and Dominant Reflectors in Random Noise Radar", International Radar Symposium, pp. 1-6, 24-26 May, 2006.

[21] Golay, M., "Complementary Series", IEEE Transactions on Information Theory, Volume 24, pp. 82-87, April, 1961.

[22] Wei, S., and Wei, C., "On the High Speed Decoding of the (23, 12, 7) Golay Code", IEEE Transactions on Information Theory, Volume 36, pp. 692-695, May, 1990.

[23] Hackett, C., "Correction to an Efficient Algorithm for Soft-Decision Decoding of the (24, 12) Extended Golay Code", IEEE Transactions on Communications, Volume 43, No. 234, pp. 812-816, February-April, 1995.

[24] Ran, M., and Snyders, J., "Constraint Designs for Maximum Likelihood Soft Decoding of RM (2, M) and the Extended Golay Codes", IEEE Transactions on Communications, Volume 43, No. 234, pp. 169-176. February-April, 1995.

[25] Harman, K., and Hodgins, B., "The Next Generation of Guidar Technology", IEEE Security Technology, IEEE 38th Annual International Conference, pp. 169-176, 11-14 Octotber, 2004.

[26] Searle, S., and Howard, S., "A Novel Polyphase Code for Side-Lobe Suppression", IEEE Waveform Diversity & Design, pp. 377-381, 8th June, 2007.

[27] Chio, R.Y., and Hao, X., "Coded Excitation for Diagonistic Ultrasound: A System Developers Perspective", IEEE Ultrasonics Symposium, pp. 437-448, 5-9 October, 2003.

[28] Hussain, A., Rais, M., and Malik, M.B., "Golay Codes in Ranging Applications", 8th IASTED Conference on Wireless and Optical Communications, pp. 159-163, Quebec City, Canada, 28-30 May, 2008.

[29] Hussain, A., and Malik, M.B., "Golay Code Based Carrier Phase Recovery", 4th IEEE International Conference on Computer and Emerging Technologies, pp. 92-97, 18-19 October, 2008.

[30] Oppenheim, A.V., Schafer, R.W., and Buck, J.R., Discrete-Time Signal Processing" 2nd Edition, Chapter-2, pp. 11, Prentice Hall, 1999.